To: Nature

A New Role for RNA G-quadruplexes in Aging and Alzheimer's Disease

[1]Lena Kallweit, [2]Eric D. Hamlett, [3]Hannah Saternos, [3]Anah Gilmore, *[3]Ann-Charlotte Granholm, *[1]Scott Horowitz

*To whom correspondence should be addressed. These two authors are co-senior authors.

[1]Department of Chemistry & Biochemistry and the Knoebel Institute for Healthy Aging, University of Denver, Denver, CO, USA.

[2]Department of Pathology and Laboratory Medicine, Medical University of South Carolina, Charleston, SC, USA

[3]Department of Neurosurgery, University of Colorado Anschutz Medical Campus, Denver, CO, USA

Summary

As the world population ages, new molecular targets in aging and Alzheimer's Disease (AD) are needed to combat the expected influx of new AD cases. Until now, the role of RNA structure in aging and neurodegeneration has largely remained unexplored. In this study, we examined human hippocampal *postmortem* tissue for the formation of RNA G-quadruplexes (rG4s) in aging and AD. We found that rG4 immunostaining strongly increased in prevalence in the hippocampus with both age and with AD severity. We further found that neurofibrillary tangles (NFTs) contained rG4s, that rG4 structure can drive tau aggregation, and that rG4 formation depended on APOE genotype in the human tissue examined. Combined with previous studies showing the dependence of rG4 structure on stress and the extreme power of rG4s at oligomerizing proteins, we propose a model of neurodegeneration in which chronic rG4 formation drives proteostasis collapse. We propose that further investigation of RNA structure in neurodegeneration is a critical avenue for future treatments and diagnoses.

As the aged population increases, Alzheimer's Disease (AD) and AD-related dementias (ADRDs) will become one of the world's largest medical and economic crises due to the lack of early diagnostic methods and durable therapies[1,2]. Age is the highest risk factor for AD, as disease prevalence increases exponentially as a function of age, and close to 40% of older adults over the age of 80 experience AD or ADRDs[3,4]. The most important genetic risk factor for developing AD is the Apolipoprotein E (APOE) genotype, where carriers of one or two copies of the APOE4 allele have a substantial increase in the risk for developing AD when compared to carriers of the APOE2 or 3 alleles[4,5]. Beyond APOE, recent meta-analyses combining genome-wide association studies (GWAS) have expanded the number of AD-risk loci[6], but most of the disease-associated variants reside in non-protein coding regions of the genome, making it difficult to elucidate how they affect AD susceptibility and pathogenesis.

The exact mechanisms behind these two predominant AD risk factors remains a mystery but both are widely associated with increased abnormal protein aggregation, which is the most abundantly observed pathological hallmark of AD pathogenesis. AD and ADRDs all have an abnormal protein aggregation profile that includes: 1) extracellular amyloid senile plaque deposition occurring at least 5-10 years before mild cognitive impairments (MCI) are observed and, 2) aggregates of phosphorylated Tau (p-Tau) forming intracellular neurofibrillary tangles (NFTs) near MCI onset[7,8]. With advancing age, protein aggregation is accelerated by the accumulation of reactive oxygen species (ROS) as well as the onset of neuroinflammation in the brain[9-11]. Having APOE4 was shown to significantly increase accumulation of amyloid and NFTs, and also increases inflammation and reactive oxygen species in the human brain[5,12]. The effects of these AD risk factors have been studied mostly at the protein level in the brain, but not yet at RNA level, where structure and function have a myriad of important roles in numerous biological processes.

RNA higher order structures of particular interest are RNA guanine-rich G-quadruplexes (rG4s)[13]. G-quadruplexes are secondary structures that can fold under physiological conditions by guanine-rich DNA and RNA molecules and occur in the genomes and transcriptomes of many species, including humans[14]. rG4s are four-stranded helices formed by guanine tetrads through Hoogsteen base-pairing, with a monovalent cation channel running down the middle of the tetrads

(Fig. 1a)[15]. G4s are involved in the regulation of DNA and RNA processes, such as replication, transcription, translation, RNA localization, and degradation. Recently, rG4s were shown to form as a function of stress in eukaryotic cells[16]. Under non-stress conditions, rG4s were largely unfolded, but upon introduction of stress (including ROS stress) the rG4s preferentially folded and remained folded until the cessation of stress[17]. This observation raises the possibility that rG4s could preferentially fold under the increased and chronic stress conditions of aging and AD in the human brain, leading to abnormally high levels of rG4 formation in older adults or in adults with protein misfolding diseases[18]. Furthermore, with recent observations that rG4s can greatly enhance protein oligomerization[19,20], the increased presence of rG4s in the brain could contribute to AD-associated aggregation. However, the presence of rG4s in the human brain or other human tissues has not been shown previously. This was the focus of the current study.

RESULTS

Formation of rG4s in aging

To determine if rG4s form in the human brain, we used the well-characterized BG4 anti-quadruplex antibody (Sigma-Aldrich MABE917, antibody null controls in Extended Data Fig. 1) to stain human hippocampal *postmortem* tissue of different ages under conditions that strongly favor cytoplasmic rG4 identification[21,22]. The tissues were obtained in collaboration with the brain bank at the Medical University of South Carolina (MUSC). The study included 19 cases, male and female, of different ages and with or without a clinical or neuropathological diagnosis of AD (see Fig. 1b). Almost all cases had received a neuropathological examination including assessment of Braak and CERAD stages according to the updated NIA criteria[7,23].

First, the rG4 staining profiles were examined at different ages, with an age range of 30-92 years of age (Fig. 1c). We discovered a significant age-related increase in rG4 immunostaining, with the densest staining observed in older individuals (Fig. 1c,d). The largest difference in staining was observed in the outer molecular layer (OML) and in the hilar region, CA4 (see Fig. 1c, legend arrows). The strongest overall staining for BG4 was found in the dentate gyrus granular cell layer (DG), but with less observable age-related increases. Staining density measurements confirmed these findings and demonstrated a highly significant increase in BG4 staining in the oldest cases

a.

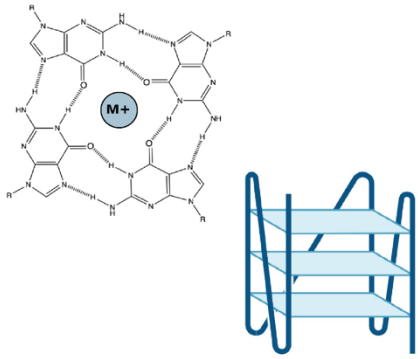

b.

Case	Gender	Age (yrs)	PMI (hrs)	Diagnosis	APOE	CERAD	BRAAK
1	F	80	23.0	Cancer	E3/E3	0	1-2
2	F	67	18.0	EOAD	E4/E4	C	6
3	F	82	6.0	Early Dementia	E3/E4	C	5
4	M	79	6.0	LOAD	E3/E4	C	5
5	F	91	3.5	LOAD	E3/E4	C	6
6	M	86	18.5	LOAD	E3/E4	C	6
7	F	85	22.0	Bipolar	E3/E3	0	0
8	M	84	11.0	Early Dementia	E4/E4	C	6
9	F	63	14.0	AD	E3/E4	C	6
10	F	90	13.0	AD	E2/E3	C	4-5
11	F	63	25.3	Poor heart function	E3/E3	0	3-4
12	M	80	7.8	LOAD	E4/E4	C	4-5
13	M	59	16.3	Control/Cardiac arrest	E3/E3	0	0
14	F	55	8.3	EOAD	E3/E4	C	4
15	M	30	11.8	Lupus	E2/E3	0	0
16	F	56	4.8	Lupus/Cancer	E3/E3	C	1-2
17	F	53	19.8	Control	E3/E3	C	1-2
18	M	74	21.3	Control	E3/E3	A	3
19	F	72	14.0	Control/Heart Failure	E3/E3	0	0

c.

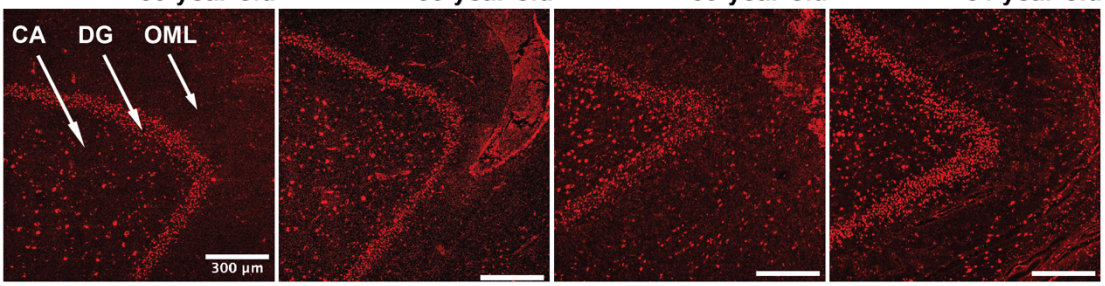

d.

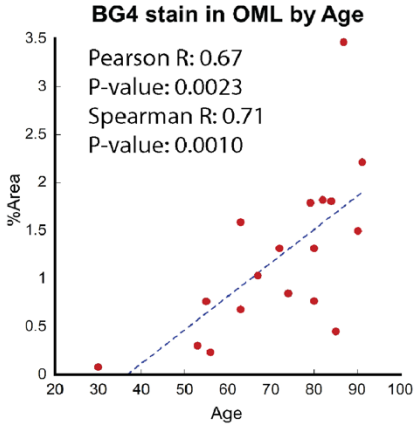

e.

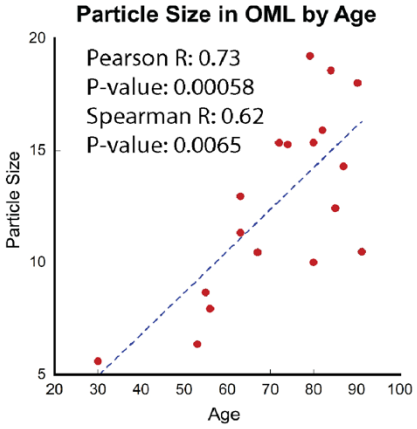

Fig 1. a, (left) Representative G-quadruplex tetrad structure with Hoogsteen base pairing stabilized by a cation at the center. (right) G-quadruplex structure with stacked tetrads. **b**, Demographics table for individuals included in this study. **c**, Immunofluorescence showing BG4 staining (red) in brain sections of human hippocampus from four control individuals of increasing age ranging 30-84 years old with no AD designation and Braak stage below 2. **d**, Correlation of percent area covered by BG4 fluorescence in the outer-molecular layer versus age of individual. **e**, Correlation of average continuous size of BG4 fluorescence versus age of individual.

studied within the OML (Fig. 1d) and the CA4 regions of cornu ammonis (Extended data Fig. 2a), confirming increased BG4 formation as a function of age. Plotting BG4 percent area versus age confirmed the observed findings and showed a strong correlation (Spearman R= 0.71) with high

significance (p= 0.0010) in the OML region (Fig. 1d). Interestingly, there was also a strong significant positive correlation between particle size and age, suggesting that larger continuous profiles of staining for rG4s were formed with aging (Spearman R= 0.62; p= 0.0065, see Fig. 1e). Positive correlations were observed between age and BG4 area in the CA4 region (Spearman R= 0.55, p= 0.018, Extended data Fig. 2a), and non-significant correlations were observed in the dentate granule cell layer. No significant correlation was found with BG4 stain and PMI (Spearman R = -0.34, p = 0.17 see Extended Data Fig. 3). In total, these data show that rG4s increased as a function of age in the human brain.

Formation of* rG4*s in AD

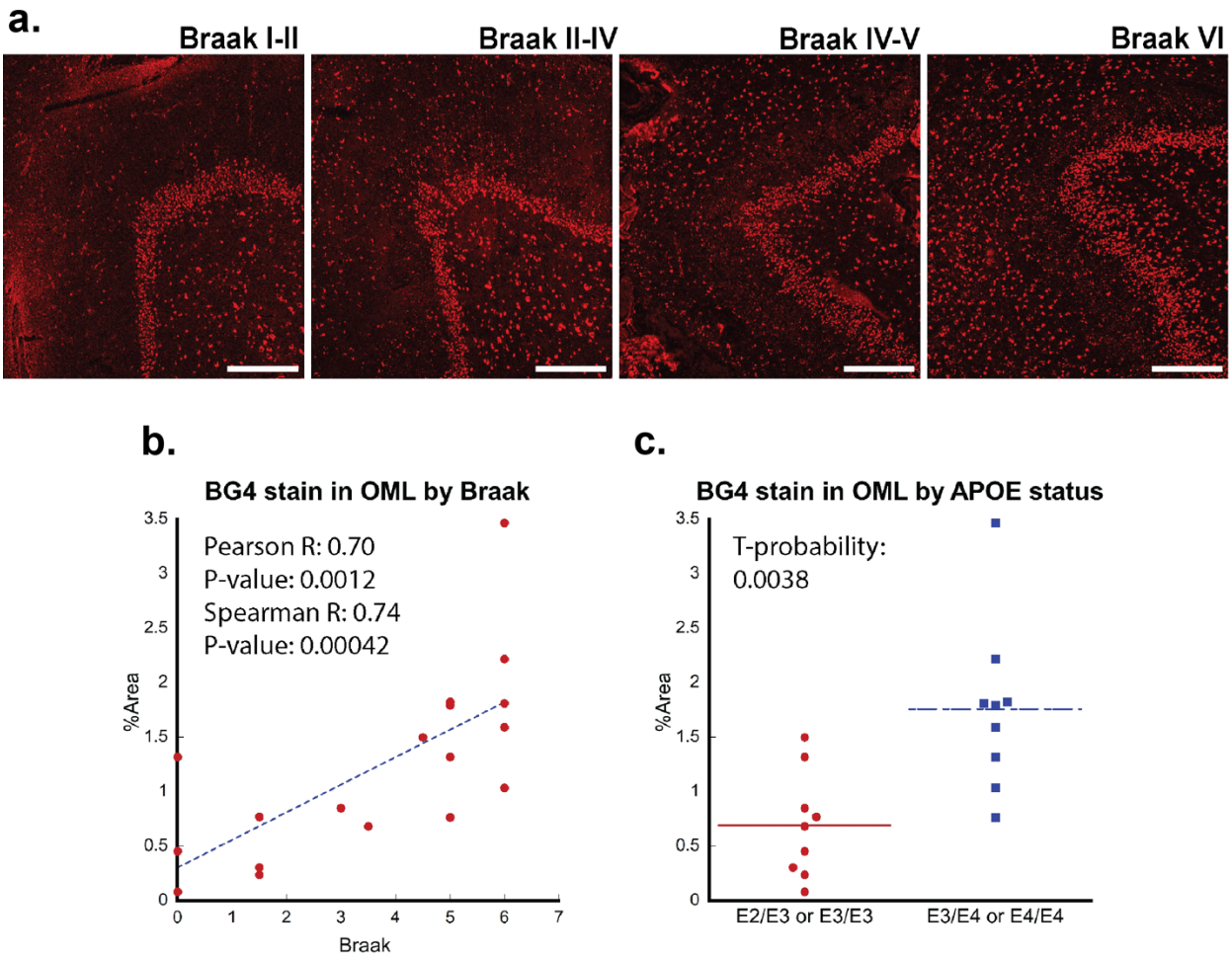

Fig 2. a, Immunofluorescence showing BG4 staining (red) in brain sections of human hippocampus with increasing Braak stage (1-6) associated with AD severity. b, Correlation of percent area BG4 coverage in the outer molecular layer versus severity of Braak stage. **c**, Quantification of percent area BG4 coverage by population with E2/E3 and E3/E3 versus E3/E4 and E4/E4 APOE alleles.

Next, we examined whether the formation of rG4s was associated with AD neuropathology. Braak staging is a neuropathological staging method that takes into account the density of neurofibrillary tangles (NFTs) both within each brain region and also from region to region[24], with higher numerical values representing greater AD severity[7]. Like in the case of aging, increased BG4 staining was readily apparent in AD cases, especially in those cases associated with a higher Braak stage (Fig. 2a). Plotting BG4 percent area versus Braak stage demonstrated a strong correlation (Spearman R= 0.74) with highly significantly increased BG4 staining with higher Braak stages ($p = 0.00042$) (Fig. 2b) in the OML region. Non-significant correlations between Braak stage severity and BG4 staining were observed within the CA4 region (Extended data fig. 2b) and dentate granule layer. Interestingly, the OML region is highly involved in AD pathology, and is a hippocampal region where AD pathology is often observed,[25] suggesting that the presence of rG4s in this particular brain region might have significance for amyloid as well as NFT formation during the AD disease process. In addition, a prominent loss of synapses in AD is found in the OML, suggesting a potential close connection with layer 2 of the entorhinal cortex[26].

If rG4 formation is more prevalent in AD than in non-AD cases and directly involved in AD pathology, we would also predict that rG4 formation would be more prevalent in APOE genotypes that are predisposed for higher LOAD risk, i.e. patients with one or two copies of the APOE4 genotype. Indeed, there was a significant increase in BG4 staining levels in the OML in *postmortem* cases with one or more APOE4 alleles compared to those with only APOE2 or APOE3 alleles (Fig. 2c). This result is consistent with a previous study performed *in vitro* in which the RNA sequences found in aggregates in different APOE genotype cell lines were different[27].

Patterns of rG4 localization

To further explore the formation of rG4s in the human hippocampus, we examined the staining pattern in different cell types based on specific antibody markers. Co-staining with markers for the most common brain cell types, rG4s were clearly abundant in neurons, oligodendrocytes, and astrocytes (Fig. 3b). rG4s exhibited no apparent colocalization with microglia (Fig. 3b). Images obtained at high magnification using a confocal microscope (Olympus) show that aggregation of BG4 immunostaining was in many cases localized in the cytoplasm near the nucleus in a punctate

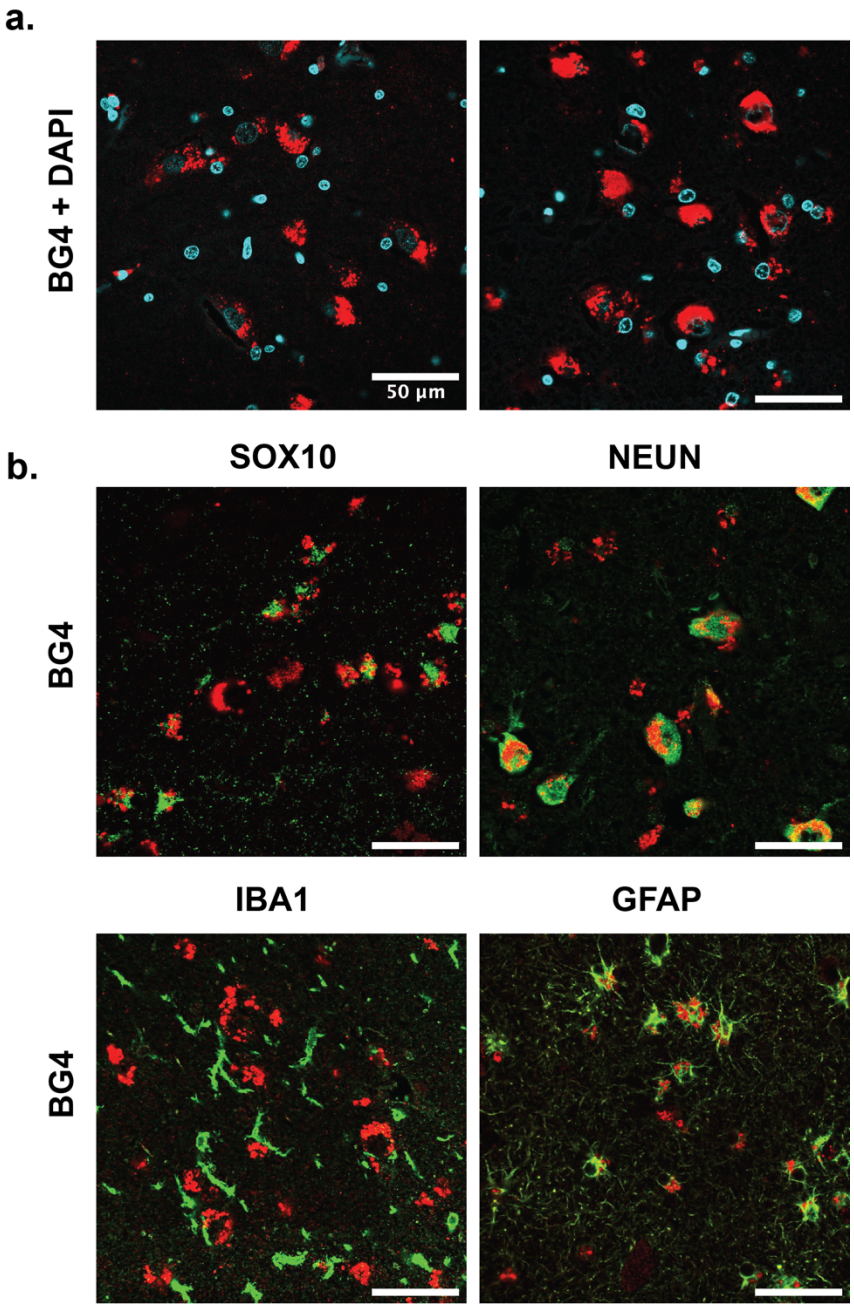

Fig 3. Cellular types and localization of rG4s. **a**, Immunofluorescence showing BG4 staining (red) in human hippocampal tissue of a 30-year-old individual with no AD pathology (left) and a 79-year-old individual with Braak stage 5 AD pathology (right). Cell nuclei stained with DAPI (blue). **b**, BG4 staining (red) with cell type markers (green). BG4 is most prevalent in oligodendrocytes (SOX10), neurons (NEUN), and astrocytes (GFAP). BG4 does not colocalize with microglia (IBA1).

pattern (Fig. 3a). This pattern is especially noticeable in the double labeling with SOX10 (Fig. 3b), which clearly shows the nuclear oligodendrocyte marker SOX10[28] staining in proximity to the cytoplasmic BG4 immunostaining.

RNA has been known to be included in AD-related aggregates of both amyloid and NFTs in patients with AD for decades[29]. rG4s can also greatly enhance protein oligomerization of many proteins[20]. A recent sequencing study of nucleic acids embedded in AD aggregates showed an enrichment in potential rG4-forming sequences[27]. Therefore, we co-stained BG4 with p-tau to

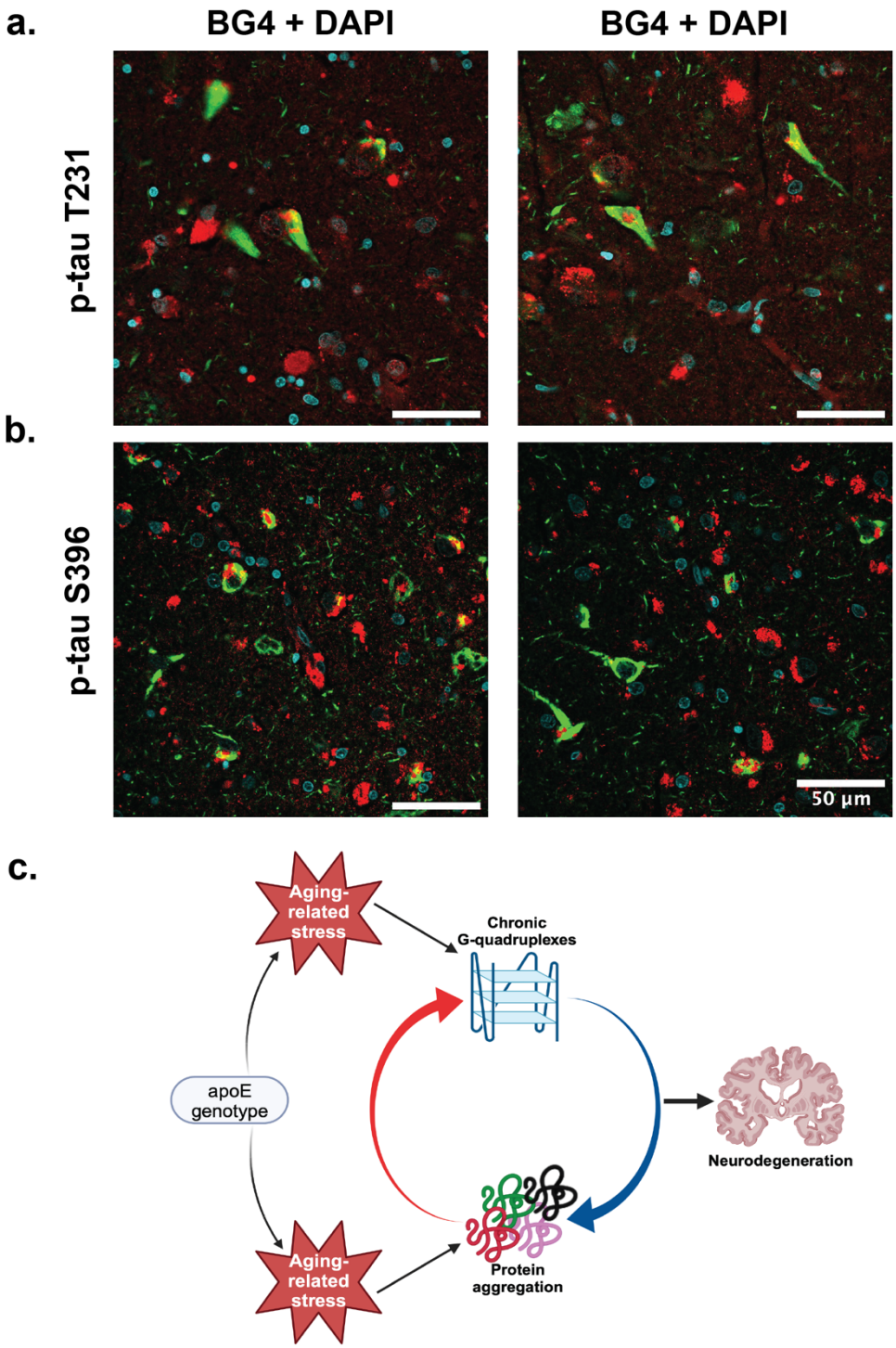

Fig 4. Colocalization of rG4s with p-tau and neurodegeneration model. a, Immunofluorescence of human hippocampus showing BG4 (red), DAPI (blue), and p-tau (green). **b**, Model relating chronic rG4 formation and protein aggregation in aging and neurodegeneration.

determine whether pathological aggregation of tau proteins co-occurred with BG4 immunostaining (Fig. 4). Indeed, we show that BG4 immunostaining co-localizes with both early and late stage

phosphorylated tau immunostaining in neurons located in the CA1-4 regions of the hippocampus (Fig. 4).

Previously, Zwierzchowski-Zarate et al explored the effects of different RNA sequences on tau aggregation in a cellular model[30]. In their study, the sequence that caused the highest level of tau aggregation was a GGGC repeat sequence[30]. However, the structure of the RNAs, including possible rG4 formation, was not explored or speculated upon. We therefore performed CD spectroscopy to determine if the sequence associated with the highest levels of tau fibrillation might be forming rG4 secondary structure. The CD spectra show that this RNA forms parallel rG4 structures *in vitro* (Extended Data Fig. 4). Combined, these findings provide evidence that in addition to accumulating in AD and aging, rG4s can template tau fibrillation more efficiently than other RNAs, co-aggregate with p-tau, and participate in the pathological hallmark of the disease.

Discussion

In this study, we demonstrated that rG4s form preferentially as a function of age and AD pathology in the human *postmortem* brain. While the granule cell layer in the dentate gyrus exhibited the most BG4 immunostaining overall, this was not an area most changed with aging and AD, as considerably stronger changes were observed in the OML and the CA4 region. rG4s were primarily found in the cytoplasm near the nucleus of neurons and oligodendrocytes and were largely found in neurons that also contained regions of positive staining against early and late-stage p-tau. Supporting this finding, a previously determined RNA sequence that strongly accelerates tau aggregation in cells was here shown to form rG4 structure. The BG4 staining levels were also impacted by APOE status, with the presence of one or two APOE4 alleles associated with higher BG4 levels in the OML region. The OML is an interesting region of the hippocampus from the pathology standpoint, since this is the region of the hippocampus exhibiting the most prominent synaptic loss early on in the disease process[26,31]. We have recently demonstrated a significant loss of presynaptic components of the OML particularly in AD[31], strengthening the findings observed herein and suggesting a particular vulnerability of this region of the hippocampus to AD progressive pathology.

Combining these observations with those previously made on the reliance of rG4 structure on cellular stress and the roles of rG4s in protein oligomerization, we can construct a model of

how rG4s form and could perpetuate the effects of AD (Fig. 4c). As ROS and other protein stresses accumulate with age and according to APOE genotype, rG4s form. Although rG4s can rescue protein folding and could release proteins when unfolded at stress cessation[32], under persistent stress proteins would not be released from the G-quadruplexes, leading to increased protein oligomerization and aggregation[20]. This function has previously been suggested for RNA in biomolecular condensates more generally[33]. The acceleration of protein oligomerization and aggregation by the rG4s could then contribute to a vicious cycle of increased aggregation, leading to synaptic loss as described recently for the OML[31].

This work raises the possibility of using rG4s as potential drug targets in AD, or given the high correlation with AD severity, as early AD biomarkers. Future work can focus on ameliorating AD symptoms through rG4 binding molecules or detecting brain-derived rG4s in exosomes. Many different rG4-binding molecules have already been created and shown to bind in human cells[34], and provide a set of promising lead compounds for potential AD treatment.

Although here we have examined only AD, there are many other aging-related diseases featuring protein aggregation, including Parkinson's Disease, ALS, and Fragile X syndrome, and Huntington's Disease. Notably, all of these diseases now have significant evidence showing rG4s as interactors with the aggregating proteins[35-47], and in the case of Fragile X, a recent study demonstrated that rG4s could contribute to its aggregation and neurotoxicity[48]. The results here combined with these previous studies suggest that the formation of rG4s could be a common mechanism of neurodegeneration.

Methods

Human brain tissue. This work was approved by the University of Colorado Institutional Review Board (IRB) and the study was performed in accordance with the ethical standards of the 1964 Declaration of Helsinki and its later amendments. However, the use of *postmortem* brain tissue for research is exempt according to federal IRB regulations and does not require IRB review and approval. All efforts were made to consider diversity, equity and inclusion (DEI) in the selection of brain tissues for this study. The tissues included in this study were obtained from the Medical University of South Carolina (MUSC) brain bank. *Postmortem* consent was obtained from the

next of kin, and the brain was rapidly removed. Fig. 1b shows the demographics for the 19 cases used for this study. The tissue was sliced in 1 cm coronal slices and subjected to free-floating fixation in 4% paraformaldehyde in PBS for 72 hours. The fixed tissue was then transferred to a 30% sucrose in phosphate buffer (PB), followed by transfer to a cryoprotection solution in PBS (30% Glycerol, 30% Ethylene Glycol and 40% PO4 Buffer) and stored in -20° C until dissection. Anatomical blocks from 19 brain regions were dissected from the 1 cm slabs, embedded in paraffin and cut at a thickness of 5µm on a Microm Microtome (Thermo Fisher Scientific Inc., Waltham, MA) and stained for routine neuropathological staging according to the NIA-AA *Revised Criteria for Diagnosis and Staging of Alzheimer's Disease* [49].

Immunofluorescence: Paraffin-embedded sections were deparaffinized in xylene (RPI, CAT#111056) and rehydrated using wash steps at: 100%, 95%, 70%, 50% ethanol followed by distilled water. Heat-induced antigen retrieval was performed using 0.05% citraconic acid at pH 7.2 for 20 minutes in a steamer. Slides were then washed with TBS and blocked with 0.25% triton-X and 5% normal serum for 1 hour. After blocking, slides were rinsed again with TBS and incubated with 1X True Black Lipofuscin Autofluorescence Quencher (Biotium CAT#23007) diluted in 70% ethanol. Slides were washed 3 times with TBS then incubated with primary antibodies listed in Extended Data Table 1 overnight, followed by Goat anti-mouse AlexaFluor 555 (Thermo Scientific #A32727) or Donkey anti-rabbit Alexafluor 488 (Invitrogen #A-21206) at 1:500 dilution for 1 hour. Slides were then washed 3 times with TBS and cover-slipped using mounting media containing DAPI (Thermo Scientific, CAT#P36931). Staining controls included omission of primary or secondary antibodies (Extended Data Fig. 1), In addition, we examined whether Braak stage correlated with aging itself (Extended Data Fig. 5). Although not significant at the 0.05 level, there is a weak correlation between Braak and Age.

Imaging and Statistical methods: Slides were imaged on a confocal microscope at 10X, 20X and 60X magnification in FTIC (green), TRITC (red) and DAPI channels. Images used for quantification were taken at constant microscope and intensity settings. All image quantification was performed using Fiji ImageJ. Background was subtracted using rolling ball radius. Images were then divided into 3 regions of interests (ROI); OML, DG and CA4. Images were submitted to an auto-threshold and particles analyzed to get a percent area measurement of BG4 staining.

These were graphed and linearly fit using Kaleidagraph using Pearson fit. Spearman and Pearson R and p-values are reported for 18 cases for age correlation and 18 cases for Braak correlation. An unpaired T-test with unequal variance was performed for the two groups E2/E3 and E3/E3 vs E3/E4 and E4/E4. All quantification was performed on 10X images obtained from an Olympus microscope.

Circular Dichroism

CD spectra were obtained using a Jasco J-1100 circular dichroism at 25°C. Sequence was resuspended in 10mM potassium phosphate pH 7.5 buffer and diluted to 12.5 μM (per strand) RNA. The CD measurement was taken from 300 nm to 190 nm at 1nm intervals using a 50 nm/min scanning speed. Parallel structure was determined using previously described spectra for quadruplex topology.[50]

Acknowledgements: Funding for this project was provided by NIH R35GM142442 to S.H., and NIH 5R01AG071228-02, R01AG070153, and R01AG061566 as well as a grant from the BrightFocus Foundation (CA2018010) to A.C.G.

Author Contributions: Idea generated by S.H., work conceptualized by S.H. and A.C.G. Experiments designed by S.H. and A.C.G, with assistance from all authors. Tissues collected and catalogued by E.D.H. Experiments performed by L.K., with assistance from H.S. and A.G. Primary writing performed by S.H., A.G.G., and L.K., with editing provided by all authors.

Authors declare no competing interests.

Literature cited

1 Collaborators, G. B. D. N. Global, regional, and national burden of neurological disorders, 1990-2016: a systematic analysis for the Global Burden of Disease Study 2016. *Lancet Neurol* **18**, 459-480 (2019). https://doi.org:10.1016/S1474-4422(18)30499-X

2 Breijyeh, Z. & Karaman, R. Comprehensive Review on Alzheimer's Disease: Causes and Treatment. *Molecules* **25** (2020). https://doi.org:10.3390/molecules25245789

3 R, A. A. Risk factors for Alzheimer's disease. *Folia Neuropathol* **57**, 87-105 (2019). https://doi.org:10.5114/fn.2019.85929

4 Hersi, M. *et al.* Risk factors associated with the onset and progression of Alzheimer's disease: A systematic review of the evidence. *Neurotoxicology* **61**, 143-187 (2017). https://doi.org:10.1016/j.neuro.2017.03.006

5 Bejanin, A. *et al.* Association of Apolipoprotein E varepsilon4 Allele With Clinical and Multimodal Biomarker Changes of Alzheimer Disease in Adults With Down Syndrome. *JAMA Neurol* **78**, 937-947 (2021). https://doi.org:10.1001/jamaneurol.2021.1893

6 Novikova, G., Andrews, S. J., Renton, A. E. & Marcora, E. Beyond association: successes and challenges in linking non-coding genetic variation to functional consequences that modulate Alzheimer's disease risk. *Mol Neurodegener* **16**, 27 (2021). https://doi.org:10.1186/s13024-021-00449-0

7 Braak, H. & Braak, E. Staging of Alzheimer's disease-related neurofibrillary changes. *Neurobiol Aging* **16**, 271-278; discussion 278-284 (1995). https://doi.org:10.1016/0197-4580(95)00021-6

8 Furman, J. L. *et al.* Widespread tau seeding activity at early Braak stages. *Acta Neuropathol* **133**, 91-100 (2017). https://doi.org:10.1007/s00401-016-1644-z

9 Bennett, R. E. *et al.* Enhanced Tau Aggregation in the Presence of Amyloid beta. *Am J Pathol* **187**, 1601-1612 (2017). https://doi.org:10.1016/j.ajpath.2017.03.011

10 Ibanez-Salazar, A. *et al.* Oxidative Stress Modifies the Levels and Phosphorylation State of Tau Protein in Human Fibroblasts. *Front Neurosci* **11**, 495 (2017). https://doi.org:10.3389/fnins.2017.00495

11 Leng, F. & Edison, P. Neuroinflammation and microglial activation in Alzheimer disease: where do we go from here? *Nat Rev Neurol* **17**, 157-172 (2021). https://doi.org:10.1038/s41582-020-00435-y

12 Raber, J., Huang, Y. & Ashford, J. W. ApoE genotype accounts for the vast majority of AD risk and AD pathology. *Neurobiol Aging* **25**, 641-650 (2004). https://doi.org:10.1016/j.neurobiolaging.2003.12.023

13 Dumas, L., Herviou, P., Dassi, E., Cammas, A. & Millevoi, S. G-Quadruplexes in RNA Biology: Recent Advances and Future Directions. *Trends Biochem Sci* **46**, 270-283 (2021). https://doi.org:10.1016/j.tibs.2020.11.001

14 Rouleau, S., Jodoin, R., Garant, J. M. & Perreault, J. P. RNA G-Quadruplexes as Key Motifs of the Transcriptome. *Adv Biochem Eng Biotechnol* **170**, 1-20 (2020). https://doi.org:10.1007/10_2017_8

15 Lyu, K., Chow, E. Y., Mou, X., Chan, T. F. & Kwok, C. K. RNA G-quadruplexes (rG4s): genomics and biological functions. *Nucleic Acids Res* **49**, 5426-5450 (2021). https://doi.org:10.1093/nar/gkab187

16 Nakanishi, C. & Seimiya, H. G-quadruplex in cancer biology and drug discovery. *Biochem Biophys Res Commun* **531**, 45-50 (2020). https://doi.org:10.1016/j.bbrc.2020.03.178

17 Kharel, P. *et al.* Stress promotes RNA G-quadruplex folding in human cells. *Nat Commun* **14**, 205 (2023). https://doi.org:10.1038/s41467-023-35811-x

18 Vijay Kumar, M. J., Morales, R. & Tsvetkov, A. S. G-quadruplexes and associated proteins in aging and Alzheimer's disease. *Front Aging* **4**, 1164057 (2023). https://doi.org:10.3389/fragi.2023.1164057

19 Masai, H. *et al.* Rif1 promotes association of G-quadruplex (G4) by its specific G4 binding and oligomerization activities. *Sci Rep* **9**, 8618 (2019). https://doi.org:10.1038/s41598-019-44736-9

20 Begeman, A. *et al.* G-Quadruplexes act as sequence-dependent protein chaperones. *EMBO Rep*, e49735 (2020). https://doi.org:10.15252/embr.201949735

21 Laguerre, A., Wong, J. M. & Monchaud, D. Direct visualization of both DNA and RNA quadruplexes in human cells via an uncommon spectroscopic method. *Sci Rep* **6**, 32141 (2016). https://doi.org:10.1038/srep32141

22 Mestre-Fos, S., Ito, C., Moore, C. M., Reddi, A. R. & Williams, L. D. Human ribosomal G-quadruplexes regulate heme bioavailability. *J Biol Chem* **295**, 14855-14865 (2020). https://doi.org:10.1074/jbc.RA120.014332

23 Jack, C. R., Jr. *et al.* An operational approach to National Institute on Aging-Alzheimer's Association criteria for preclinical Alzheimer disease. *Ann Neurol* **71**, 765-775 (2012). https://doi.org:10.1002/ana.22628

24 Trejo-Lopez, J. A., Yachnis, A. T. & Prokop, S. Neuropathology of Alzheimer's Disease. *Neurotherapeutics* **19**, 173-185 (2022). https://doi.org:10.1007/s13311-021-01146-y

25 Dong, H., Martin, M. V., Chambers, S. & Csernansky, J. G. Spatial relationship between synapse loss and beta-amyloid deposition in Tg2576 mice. *J Comp Neurol* **500**, 311-321 (2007). https://doi.org:10.1002/cne.21176

26 Lassmann, H., Fischer, P. & Jellinger, K. Synaptic pathology of Alzheimer's disease. *Ann N Y Acad Sci* **695**, 59-64 (1993). https://doi.org:10.1111/j.1749-6632.1993.tb23028.x

27 Shmookler Reis, R. J. *et al.* "Protein aggregates" contain RNA and DNA, entrapped by misfolded proteins but largely rescued by slowing translational elongation. *Aging Cell*, e13326 (2021). https://doi.org:10.1111/acel.13326

28 Turnescu, T. *et al.* Sox8 and Sox10 jointly maintain myelin gene expression in oligodendrocytes. *Glia* **66**, 279-294 (2018). https://doi.org:10.1002/glia.23242

29 Wolozin, B. & Apicco, D. RNA binding proteins and the genesis of neurodegenerative diseases. *Adv Exp Med Biol* **822**, 11-15 (2015). https://doi.org:10.1007/978-3-319-08927-0_3

30 Zwierzchowski-Zarate, A. N. *et al.* RNA induces unique tau strains and stabilizes Alzheimer's disease seeds. *J Biol Chem* **298**, 102132 (2022). https://doi.org:10.1016/j.jbc.2022.102132

31 Haytural, H. *et al.* Distinctive alteration of presynaptic proteins in the outer molecular layer of the dentate gyrus in Alzheimer's disease. *Brain Commun* **3**, fcab079 (2021). https://doi.org:10.1093/braincomms/fcab079

32 Son, A., Huizar Cabral, V., Huang, Z., Litberg, T. J. & Horowitz, S. G-quadruplexes rescuing protein folding. *Proc Natl Acad Sci U S A* **120**, e2216308120 (2023). https://doi.org:10.1073/pnas.2216308120

33 Mateju, D. *et al.* An aberrant phase transition of stress granules triggered by misfolded protein and prevented by chaperone function. *Embo J* **36**, 1669-1687 (2017). https://doi.org:10.15252/embj.201695957

34 Zheng, B. X. *et al.* Structurally diverse G-quadruplexes as the noncanonical nucleic acid drug target for live cell imaging and antibacterial study. *Chem Commun* **59**, 1415-1433 (2023). https://doi.org:10.1039/d2cc05945b

35 Imperatore, J. A., McAninch, D. S., Valdez-Sinon, A. N., Bassell, G. J. & Mihailescu, M. R. FUS Recognizes G Quadruplex Structures Within Neuronal mRNAs. *Front Mol Biosci* **7**, 6 (2020). https://doi.org:10.3389/fmolb.2020.00006

36 Ishiguro, A. *et al.* Molecular dissection of ALS-linked TDP-43 - involvement of the Gly-rich domain in interaction with G-quadruplex mRNA. *Febs Lett* **594**, 2254-2265 (2020). https://doi.org:10.1002/1873-3468.13800

37 Liu, X. & Xu, Y. HnRNPA1 Specifically Recognizes the Base of Nucleotide at the Loop of RNA G-Quadruplex. *Molecules* **23** (2018). https://doi.org:10.3390/molecules23010237

38 Mori, K. *et al.* hnRNP A3 binds to GGGGCC repeats and is a constituent of p62-positive/TDP43-negative inclusions in the hippocampus of patients with C9orf72 mutations. *Acta Neuropathol* **125**, 413-423 (2013). https://doi.org:10.1007/s00401-013-1088-7

39 Oyoshi, T. & Kurokawa, R. Structure of noncoding RNA is a determinant of function of RNA binding proteins in transcriptional regulation. *Cell Biosci* **2**, 1 (2012). https://doi.org:10.1186/2045-3701-2-1

40 Scalabrin, M. *et al.* The cellular protein hnRNP A2/B1 enhances HIV-1 transcription by unfolding LTR promoter G-quadruplexes. *Sci Rep* **7**, 45244 (2017). https://doi.org:10.1038/srep45244

41 Takahama, K., Kino, K., Arai, S., Kurokawa, R. & Oyoshi, T. Identification of Ewing's sarcoma protein as a G-quadruplex DNA- and RNA-binding protein. *FEBS J* **278**, 988-998 (2011). https://doi.org:10.1111/j.1742-4658.2011.08020.x

42 Liu, W. *et al.* A DNA G-quadruplex converts SOD1 into fibrillar aggregates. *Chinese Chemical Letters* (2021). https://doi.org:https://doi.org/10.1016/j.cclet.2021.01.045

43 Mejzini, R. *et al.* ALS Genetics, Mechanisms, and Therapeutics: Where Are We Now? *Front Neurosci* **13**, 1310 (2019). https://doi.org:10.3389/fnins.2019.01310

44 Guerrero, E. N. *et al.* TDP-43/FUS in motor neuron disease: Complexity and challenges. *Prog Neurobiol* **145-146**, 78-97 (2016). https://doi.org:10.1016/j.pneurobio.2016.09.004

45 Riccardi, C. *et al.* Fighting the Huntington's Disease with a G-Quadruplex-Forming Aptamer Specifically Binding to Mutant Huntingtin Protein: Biophysical Characterization, In Vitro and In Vivo Studies. *Int J Mol Sci* **23** (2022). https://doi.org:10.3390/ijms23094804

46 Goering, R. *et al.* FMRP promotes RNA localization to neuronal projections through interactions between its RGG domain and G-quadruplex RNA sequences. *Elife* **9** (2020). https://doi.org:ARTN e52621
10.7554/eLife.52621

47 Matsuo, K. *et al.* RNA G-quadruplexes forming scaffolds for α-synuclein aggregation lead to progressive neurodegeneration. *bioRxiv*, 2023.2007.2010.548322 (2023). https://doi.org:10.1101/2023.07.10.548322

48 Asamitsu, S. *et al.* CGG repeat RNA G-quadruplexes interact with FMRpolyG to cause neuronal dysfunction in fragile X-related tremor/ataxia syndrome. *Sci Adv* **7** (2021). https://doi.org:10.1126/sciadv.abd9440

49 Hyman, B. T. *et al.* National Institute on Aging-Alzheimer's Association guidelines for the neuropathologic assessment of Alzheimer's disease. *Alzheimers Dement* **8**, 1-13 (2012). https://doi.org:10.1016/j.jalz.2011.10.007

50 Cheng, M. *et al.* Loop permutation affects the topology and stability of G-quadruplexes. *Nucleic Acids Res* **46**, 9264-9275 (2018). https://doi.org:10.1093/nar/gky757

Antibody	**Host**	**Source**	**Dilution**
BG4	E.Coli monoclonal	Sigma-Aldrich MABE917	1:250
Anti-flag M2	Mouse monoclonal	Sigma-Alrich F1804	1:500
NeuN	Rabbit monoclonal	Cell Signaling 12943S	1:1000
Phospho-tau Ser396	Rabbit polyclonal	Invitrogen 44-752G	1:500
Phospho-tau T231	Rabbit polyclonal	Invitrogen 44-746G	1:500
SOX10	Rabbit monoclonal	Abcam ab155279	1:500
GFAP	Rabbit polyclonal	Abcam EPR1034Y	1:500
IBA1	Rabbit polyclonal	WAKO 013-27691	1:1000

Extended Data Table 1. Antibodies used in the study and their respective dilutions and sources.

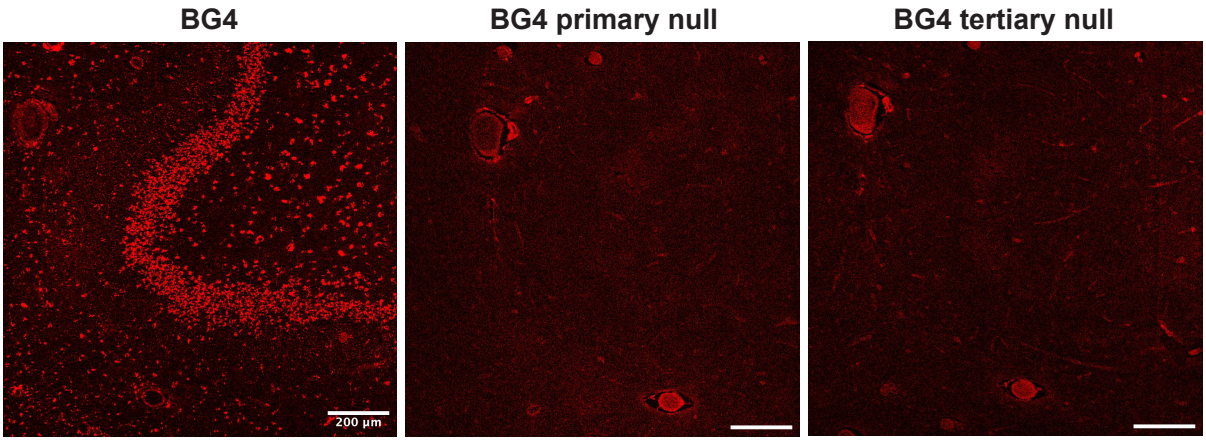

Extended Data Fig 1. Antibody null controls. (left) Complete BG4 staining for comparison. (center) BG4 primary null in incubated with intermediate and tertiary antibodies only. (right) BG4 tertiary null is incubated with primary and intermediate antibodies only.

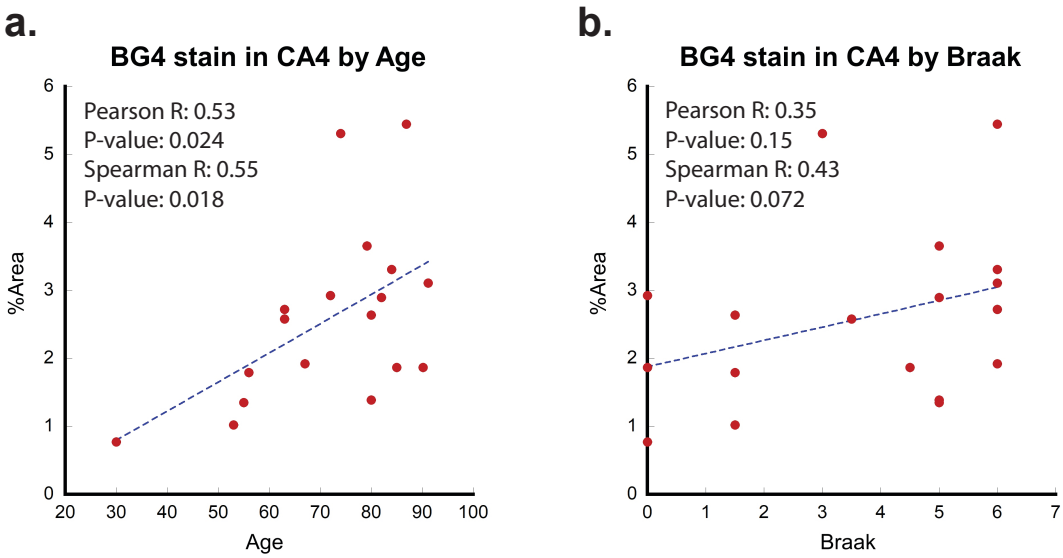

Extended Data Fig 2. a, BG4 stain in the CA4 region correlates with age. **b,** BG4 exhibits weak, nonsignificant correlation with Braak stage in CA4 region.

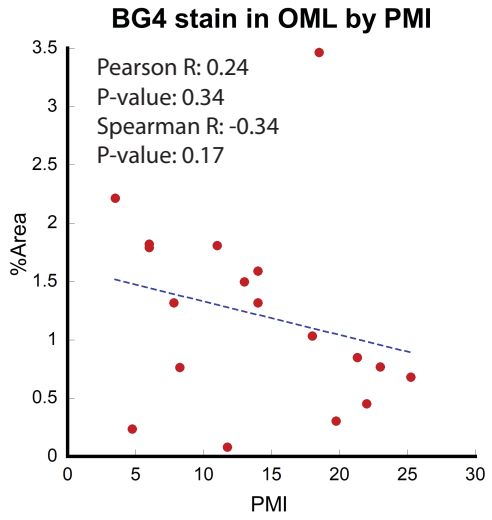

Extended Data Fig 3. No significant correlation observed between BG4 stain and PMI.

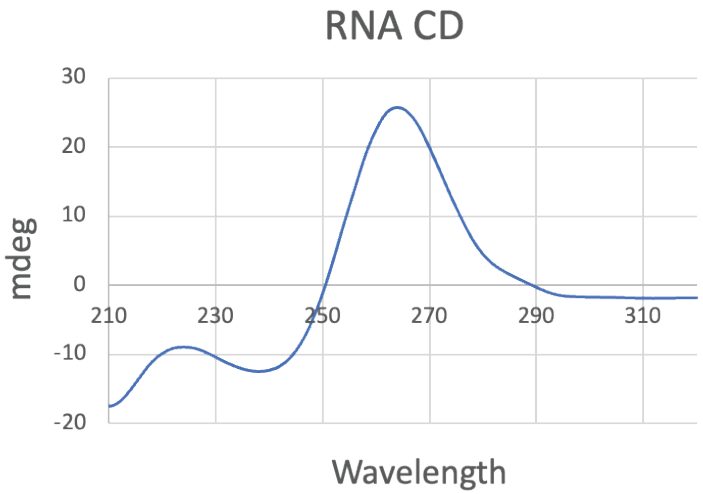

Extended Data Fig 4. Circular dichroism spectra showing G-quadruplex structure of RNA sequence able to most efficiently template tau fibrillization.

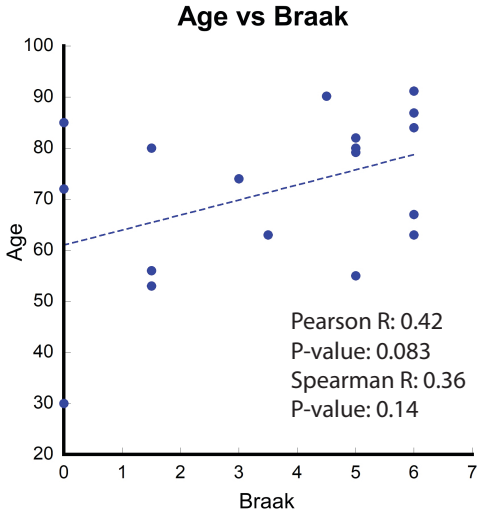

Extended Data Fig 5. Although not significant at the 0.05 level, weak correlation was observed between age and Braak stage.